*Int. J. Rock Mech. Min. Sci.* Vol. 5, pp. 415–426. Pergamon Press 1968. Printed in Great Britain

# A TEST OF THE LAW OF EFFECTIVE STRESS FOR CRYSTALLINE ROCKS OF LOW POROSITY

W. F. BRACE and R. J. MARTIN, III

Department of Geology and Geophysics, Massachusetts Institute of Technology, Cambridge, Mass.

(*Received 5 January* 1968)

**Abstract**—A variety of crystalline silicate rocks of low porosity (0·001–0·03) were fractured in triaxial experiments at strain rates from about $10^{-3}$ to $10^{-8}$ sec$^{-1}$. Comparison of the fracture strengths at different pore pressures provided a test of the law of effective stress for these brittle rocks.

The tests revealed that the law of effective stress held for these rocks only when loading rate was less than some critical value which depended on permeability of the rock, viscosity of the pore fluid and sample geometry. In our experiments with water, it was about $10^{-7}$ sec$^{-1}$ for cylindrical samples of granite several centimeters long for example. In experiments at loading rates greater than the critical value, the rock was as much as 50 per cent stronger than at zero pore pressure. Although this effect will probably have little geologic application, it could well be significant for rock stressed as a result of earthquake motion or for rock in the vicinity of buried nuclear explosions.

## INTRODUCTION

THERE is ample evidence that the law of effective stress holds for many rocks [1]. In essence, this law states that mechanical behavior of a porous solid depends uniquely on the effective stress, which is the difference between the total normal stress active on any plane through the solid, and the pressure of fluids in the pores. This is an important law, for most rocks below a very shallow depth are probably saturated with fluids. Also, a wide range of properties depend on the effective stress or effective confining pressure which is exerted on a rock. Fracture strength and ductility, not unexpectedly, depend on effective confining pressure [2–4]. Elastic modulus and sound velocity do as well, at low pressures. Electrical resistivity of water-saturated rocks [5], thermal conductivity [6], and even permeability [7] may, in some rocks, depend uniquely on the effective confining pressure.

The law of effective stress may not hold universally, however. HEARD [8] noted that the brittle–ductile transition of Solenhofen limestone was virtually independent of pore pressure. And, according to HANDIN *et al.* [3], the deformation of a crystalline marble and a dolomite also failed to show the usual dependence on effective rather than total stress. This was believed to be due to the low porosity of these three rocks; the porosity was only a few per cent. Low porosity implies low permeability and, in rocks of low permeability, fluid may not completely permeate the pore space. This is necessary in order that the pore pressure be transmitted throughout the rock and be fully effective in reducing the total stress.

One important class of rocks, the crystalline silicates, has received little attention in studies of the effect of pore fluids. Based on the results given above one might predict that these rocks too, because of low porosity, would not obey the law of effective stress. To explore this possibility we decided to measure fracture strength of a suite of typical brittle silicate rocks. Fracture strength is a property which can be measured easily and with some precision, even in triaxial experiments; furthermore, it is very sensitive to the effective confining pressure. It was clear that we would need to vary loading rate in our experiments, for if agreement with the law depended on the ease with which pore fluids could move in and out of a rock, then we might expect agreement with the law for a slow loading rate and disagreement if we loaded rapidly. It would be interesting to know the critical loading rate, or strain rate, at which the law might break down for typical crystalline rocks.

## EXPERIMENTAL METHOD

We made our test of the effective stress law in the following way. We selected one set of pressures at which all experiments would be done and then compared fracture strengths with and without pore pressure at different strain rates. Specifically, we compared the strength at zero pore pressure and 1·56 kb confining pressure with the strength at 1·56 kb pore pressure and 3·12 kb confining pressure, at the same strain rate. We repeated this at a series of strain rates over the range $10^{-3}$ to $10^{-8}$ per sec. To explore the effect of fluid viscosity we used three different fluids, water, acetone, and a Dow Corning silicone fluid which was 600 times more viscous than water (Table 1). For two of the rocks, Maryland diabase and Westerly granite, we compared the strengths of dry rock (dried for 24 hr *in vacuo* at 120°C, then exposed for several days to laboratory atmosphere of 40 per cent relative humidity) with rock which was saturated with water but maintained during an experiment at zero pore pressure. These two situations are referred to below as *dry* and *saturated*, respectively.

The rocks studied were granite, diabase, fine-grained dolomite rock, gabbro, partly serpentinized dunite, and silica-cemented sandstone. The properties are summarized in Table 2. The porosities shown deserve comment. We show in Table 2 the porosity at the conditions of the triaxial experiments. At 1·5 kb confining pressure, most pre-existing cracks

TABLE 1. PROPERTIES OF FLUIDS

Values given are for 30°C and 1500 bars pressure. Compressibilities are taken from [9] and viscosities from [10]. We assumed that the effect of pressure on compressibility and viscosity was the same for silicone fluid 200–50 as for 200–100. Absolute viscosity of water at 0°, 1 bar, was assumed to be 1·79 cp, and absolute viscosity of acetone at 30°C, 1 bar, to be 0·295 cp

| Fluid | Compressibility ($10^{-6}$ bars$^{-1}$) | Viscosity (cp) |
|---|---|---|
| Water | 32 | 0·95 |
| Acetone | 44 | 0·58 |
| Silicone fluid, 200–50 | 39 | 620·0 |

are closed, so that we may assume that crack porosity [6] was zero. Pore porosity remained and this is the figure given in Table 1. Uncertainty in porosity is about 0·001, so that the rocks shown with zero porosity may well have a porosity of as high as 0·001.

Not all of the rocks were studied in the same detail. A general pattern of behavior was established with Maryland diabase, the granite and the sandstone. We assumed that this pattern was followed by the other rocks and did only three experiments for each; three is the minimum number required to define the pattern.

TABLE 2. ROCK PROPERTIES

| Rock | Density ($g/cm^3$) | $d$ (mm) | Porosity | Modal analysis |
|---|---|---|---|---|
| Granite, Westerly, Rhode Island | 2·646 | 0·75 | 0·007 | 27·5 qu<br>35·4 mi<br>31·4 $an_{17}$<br>4·9 mica |
| Diabase, Frederick, Maryland | 3·029 | 0·175 | 0 | 48 $an_{47}$<br>49 au<br>1 mica |
| Blair Dolomite, West Virginia | 2·847 | 0·075 | 0·001 | 85 do<br>6 ca<br>9 insol. residue |
| Gabbro, San Marcos California | 2·819 | 2·0 | 0·002 | 70 $an_{43}$<br>8 au<br>7 am<br>12 mica<br>3 ox |
| Diabase, Columbia North Carolina | 2·979 | 0·75 | 0 | 62 $an_{55}$<br>22 au<br>11 ol<br>4 ox<br>1 mica |
| Dunite, Spruce Pine North Carolina | 3·262 | 0·5 | 0·001 | 96 ol<br>3 serp<br>1 ox |
| Sandstone (Pottsville) Spring City, Tenn. | 2·620 | 0·2 | 0·026 | 46 qu<br>41 or<br>11 mica<br>2 ox |

Abbreviations:

| | | | |
|---|---|---|---|
| qu | quartz | do | dolomite |
| mi | microcline | ca | calcite |
| $an_{17}$ | plagioclase with anorthite content | ol | olivine |
| | | serp | serpentine |
| au | augite | or | orthoclase |
| am | amphibole | ox | oxides |

Strength was determined in a triaxial experiment similar to that used by HANDIN *et al.* [3]. A cylinder of rock 1·58 cm in diameter and 3·81 cm long was subjected to confining pressure through a 3-mm thick polyurethane tubular jacket. Pore fluids had access to one end of the sample through a hollow piston. The piston was driven at constant rate by a ball screw mechanism [11]. Axial force, measured externally, was determined with a probable error of 2 per cent. Pore pressure, as indicated on a gage, and confining pressure were held constant by manual adjustments during an experiment; at strain rates slower than $10^{-3}$, pressure could be maintained to within a few bars of the desired value. At $10^{-3}$, fluctuations could have been as much as 20 bars. Aside from these fluctuations, probable error of the pressures we report is about 1 per cent.

## OBSERVATIONS

The results are given in Figs. 1–4, in which strength which is equivalent to stress difference at fracture is plotted for the different strain rates and fluids.

The difference in strength between water-saturated and dry samples for both granite (Fig. 1) and Maryland diabase (Fig. 2) was about 1 per cent. With one exception, the

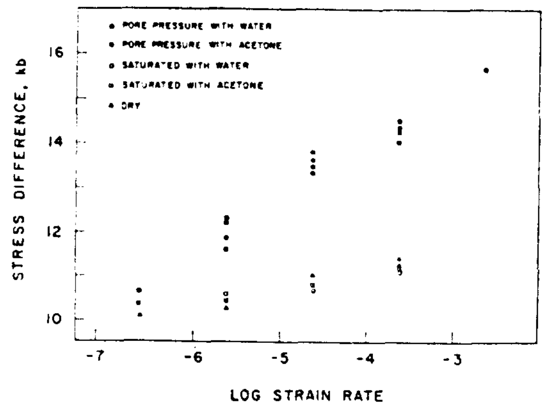


Fig. 1. Strength of Westerly granite as a function of strain rate.

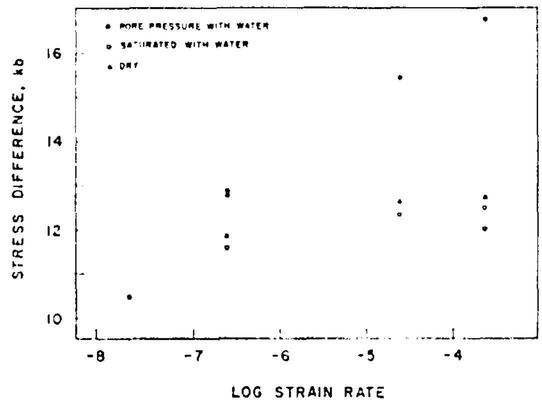


Fig. 2. Strength of Maryland diabase as a function of strain rate.

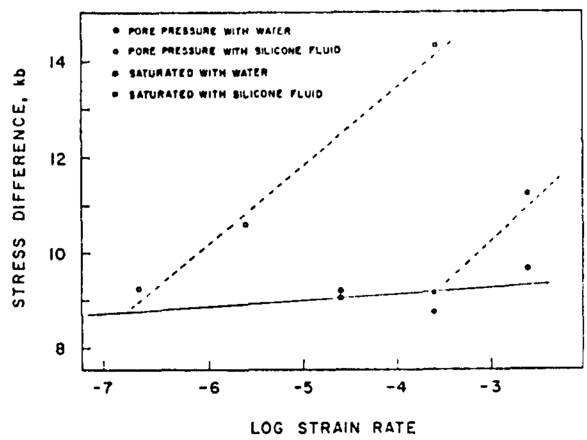


Fig. 3. Strength of sandstone as a function of strain rate for two different pore fluids.

strength of the dry samples was greater than the saturated ones at a given strain rate. However, strength of both dry and water-saturated samples decreased somewhat with decreasing strain rates. For both granite and diabase this decrease amounted to about 8 per cent for a thousandfold decrease in strain rates. For granite, the decrease with acetone as the fluid was essentially the same as for water.

An interesting effect accompanied nearly all of the tests with pore pressure. That is, strength with pore pressure was greater than for saturated or dry rock. Furthermore, this increase in strength became larger at the more rapid strain rates. The increase amounted to

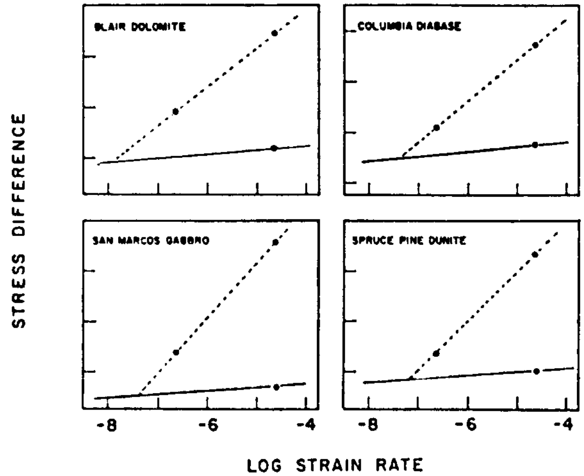


FIG. 4. Strength of four rocks as a function of strain rate.

as much as 50 per cent over the value at zero pore pressure. For one rock, the sandstone (Fig. 3) behavior clearly varied with the two fluids used. With silicone oil, we observed the typical sharp increase in strength with strain rate seen in the other rocks with water (Figs. 1, 2, 4). With water as the pore fluid, strength agreed with saturated values at slow rates ($10^{-4}$ and $10^{-6}$) but showed an increase at a high rate ($10^{-3}$ sec$^{-1}$). Disagreement of the two $10^{-3}$ values for sandstone reflects some bending in the sample corresponding to the lower value.

The machine used for the experiments, as it was mechanically rather than hydraulically driven, had a high stiffness (about $10^{6}$ kg cm$^{-1}$). This together with the tough, virtually indestructible jacketing material insured that nearly all samples were recovered more or less intact. We could, therefore, see any effect of strain rate and of pore pressure on the pattern of fractures.

Typically, a sample was cut by a single major fault, along which a small shear displacement had occurred. The inclination of this fault to the direction of maximum compression was 30° $\pm$ 3; there was no apparent difference in angle between samples fractured with pore pressure and those fractured dry or saturated. Although there was typically a single throughgoing fault, many small fractures were common. These were parallel or conjugate to the main fault, and the length ranged up to half that of the main fault. Although the density of these small fractures varied somewhat from sample to sample, there was no obvious correlation of fracture density with either strain rate or with pore pressure. The major fault typically intersected one of the end surfaces of the sample near a corner; there was no obvious preference for that corner near the fluid reservoir, except a few of the runs at high strain rate with pore pressure. There, as one might anticipate, the end nearest the source of fluid seemed to be the end from which the main fracture emanated. To sum up, there seemed to be little in the pattern of fracturing which might correlate with either strain rate or the presence of a fluid under pressure. Of course, we observed surface features only (through the transparent jacket); more thorough study of fractures within the sample might still reveal significant differences in density, spacing or distribution of the many subsidiary fractures.

One reason that we had suspected a difference in fracture pattern at different strain rates was the disappearance of the sudden stress drop in certain of our experiments. Typically, fracture of all of our rocks was accompanied by a pronounced sudden stress drop. However, no sudden stress drop accompanied the fracture of samples which were subject to pore pressure and which were strained at $10^{-6}$ sec$^{-1}$ or slower. When the maximum stress was attained in these samples the load fell slowly and steadily; a drop of about 25 per cent occurred in 3 to 4 min. Inspection of the sample revealed a single pronounced fault different in no obvious way from faults in samples which failed suddenly.

## DISCUSSION

We may generalize our results in a way which emphasizes the important features. In Fig. 5 we show the behavior we infer for all of our rocks. It is the behavior which we believe we would have observed for a given rock had we been able to conduct experiments over a wider range of strain rates. We were not able to do so for several reasons. We could not run an experiment at a faster rate than $10^{-3}$ sec$^{-1}$ and still hold pore and confining pressure constant. It was inconvenient to run an experiment at rates slower than $10^{-8}$ sec$^{-1}$ because of the time required; at $10^{-8}$ sec$^{-1}$, an experiment requires over a week.

The solid curve in Fig. 5 represents the strength of dry or saturated rock. Its principal feature of interest is the slight decrease in strength with decreasing loading rate. The decrease

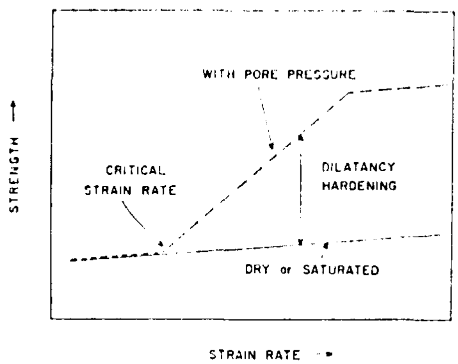


FIG. 5. Generalized dependence of strength on strain rate for a given pore fluid.

we observe is similar to that reported elsewhere [4]. The reasons for the decrease are not clear. It might be attributed to the corrosive effects of the pore fluids or water vapor, but if this is so, then it is hard to explain why the effects of water and acetone seem to be similar for granite. Also, it is to be noted that strengths of water-saturated and dry granite differ but little. Perhaps it is best, until more is known about what actually happens when rocks fracture, to forego further speculation about the causes of this slope.

The dotted curve in Fig. 5 represents strengths of samples with pore pressure. The curve has three parts, a toe at slow strain rates which coincides with the saturated curve, a steep slope at intermediate strain rates, and a 'shelf' at high strain rates which is parallel with the saturated curve. The first two parts of this curve are derived from our observations here, the shelf, on the basis of interpretation of our observations. Thus, the middle, sloping region, which extends down to join the saturated curve, is seen in Figs. 1–4. The toe of the curve, where saturated and pore pressure values coincide, is seen when water was used for the pore fluid with sandstone.

We call the strain rate at which the two curves first coincide the *critical strain rate*. For all of the rocks except sandstone it fell between $10^{-8}$ and $10^{-7}$ $sec^{-1}$. For sandstone with silicone oil it also fell in this range; for sandstone with water it was $10^{-4}$ $sec^{-1}$ or higher. It is unlikely that the change in slope is as sharp as shown in Fig. 5; however, details of the actual transition are not available.

To what is the apparent strengthening effect of rapid loading to be attributed in our tests with pore pressure? Almost certainly, the effect must be due in part to dilatancy. Nearly all rocks as well as concrete [12, 1] become dilatant prior to fracture in compression, even under high confining pressure. Dilatancy represents an increase in porosity, and changes in porosity will lead to changes in pore pressure. Although pore pressure, as measured on an external gage, was maintained constant during our experiments, pore pressure within our samples could have changed. Particularly at fast loading rates, changes in pore pressure within our samples probably lagged behind changes in the external part of the pore fluid system. On the other hand, at slow loading rates changes in pore pressure brought about by dilatancy might well have been communicated throughout the system; constant pore pressure at the gage could have very nearly corresponded to constant pore pressure within the sample.

The cause of the strengthening lies in the fact that nearly all rocks become stronger with an increase in effective confining pressure. Since effective confining pressure is confining pressure minus pore pressure, then as pore pressure drops due to dilatancy, effective confining pressure increases. The more rapid the loading rate, the greater the drop in pore pressure within the sample, the greater the increase in effective confining pressure, and the greater the stress difference which the rock could support. Qualitatively this accounts for the middle, sloping region in Fig. 5. At the critical strain rate, changes in pore pressure in the sample just keep pace with those in the external system. The shelf in the dotted curve must be present inasmuch as pore pressure cannot drop indefinitely; when it is near zero, no further strengthening is possible regardless of the rate of loading.

FRANK [14] used the term *dilatancy hardening* for the phenomenon we describe above. Although he referred to sand, evidently the term is applicable here.

To judge from the results for sandstone (Fig. 3) the amount of dilatancy hardening depended on the fluid we used to apply pore pressure. This fact, too, lends support to our explanation. If strengthening depends on the pressure difference which develops between internal and external parts of the pore fluid system, then this difference will clearly depend on permeability of the rock and discosity of the fluid, and perhaps on other factors such as sample length, or the presence of reservoirs of fluid at both ends. As we increase fluid viscosity in a given rock, the pressure difference at a given strain rate will increase, and the amount of dilatancy hardening will increase. Also the critical strain rate will shift to slower rates with higher viscosity. Thus, neither the degree of dilatancy hardening nor the critical strain rate at which hardening begins depend solely on the rock, but depend as well on factors such as fluid viscosity and distances from the rock mass in question to a source of fluid.

We may gain further insight into the mechanism of dilatancy hardening by an approximate analysis [15]. This is based on the mechanism described above and on certain simplifying assumptions and boundary conditions. We wish to calculate two things, the critical strain rate for hardening, and the actual amount of hardening. This is done by calculation of the actual pore pressure inside the rock sample just before fracture. From this we can estimate the amount of dilatancy hardening. This was done for Westerly granite, for which most of the required information is available. As shown in the Appendix, volume change and permeability must be known as a function of stress; in addition, we need to know strength as a function of effective confining pressure.

The results of the analysis carried out in the Appendix are given in Fig. 6, in which we show calculated pore pressure as a function of the strain rate. In our experiments pore pressure was initially set at 1565 bars; as shown in Fig. 6 the actual pore pressure may fall

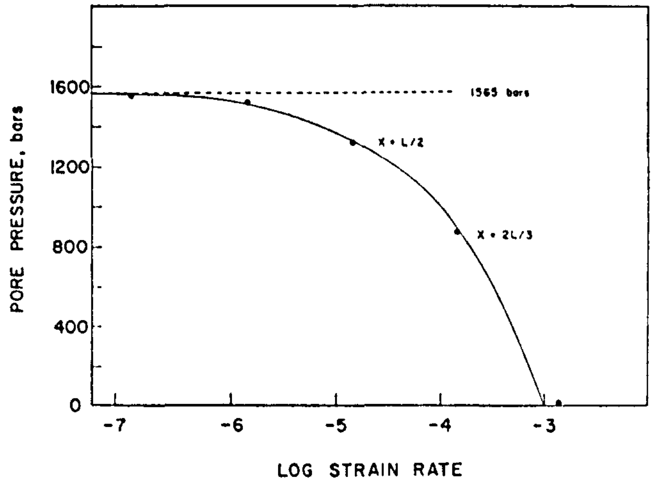


FIG. 6. Calculated pore pressure for Westerly granite at different strain rates. It is assumed that pressure was 1565 bars before stress was applied, at all strain rates. Each point was calculated as described in the Appendix. The value of $x$ given is the point in the sample for which the calculation was made.

well below this. Near $10^{-3}$ sec$^{-1}$, it will be close to zero; near $10^{-7}$ it will remain essentially unchanged. Based on this, the critical strain rate for dilatancy hardening would be near $10^{-7}$ sec$^{-1}$.

Data for the dependence of strength on effective confining pressure [12] can next be used to compare observed values with the theoretical strength this rock should have if the pore pressure changes shown in Fig. 6 did in fact occur. Predicted and observed strengths are compared in Fig. 7. For clarity the observed values have been referred to a saturated curve of zero slope.

The agreement between predicted and observed values in Fig. 7 is quite good. Critical strain rate has been predicted to within about an order of magnitude, and magnitude of the dilatancy to a factor of two or better at the higher strain rates.

Equation (2) in the Appendix suggests how factors such as length and fluid properties might affect the critical strain rate. Other things being equal, critical strain rate ought to be

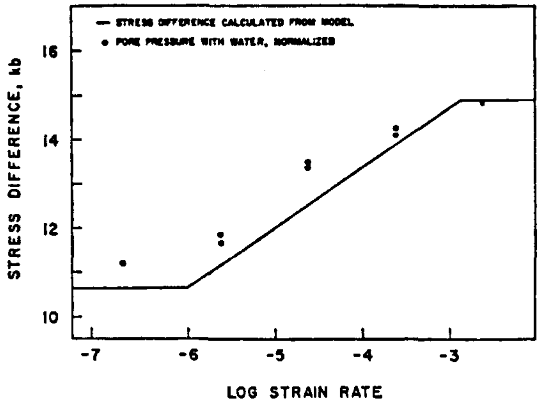


FIG. 7. Calculated vs. observed strength for Westerly granite as a function of strain rate. The values of strength are referred to a saturated curve of zero slope.

inversely proportional to the product of viscosity and compressibility of the pore fluid. We can test this prediction with data for the sandstone (Fig. 3). From Table 1 this product differs for water and silicone oil by about a factor of 600. From Fig. 3, it is seen that the critical rates for water and silicone oil differ by about a factor of 1000. Considering the uncertainties in location of the toe of the slope in Fig. 3 and uncertainties in the properties of the oil used, we conclude that the data are at least consistent with our theory.

To return to the question posed at the outset of this study, we have, to the extent that Fig. 5 represents general behavior of dense crystalline rocks, a clear answer. At strain rates slower than the critical strain rate the law of effective stress holds. At faster rates the law does not hold. The actual value of the critical strain rate was $10^{-7}$ to $10^{-8}$ $sec^{-1}$ for most of the rocks when water was the pore fluid.

To apply our results geologically, actual geologic strain rates and actual dimensions must be specified. The effect of dimension can be estimated from the way in which sample length appears in our analysis. As shown in equation (2) of the Appendix, the pressure at any given time varies as length squared. Our experimental samples had dimensions on the order of a centimeter; other things being equal, the critical strain rate for rocks masses with dimensions on the order of a meter might therefore be $10^4$ times slower than the rate for our small samples. Various estimates of geologic strain rates yield values of $10^{-14}$ $sec^{-1}$ or slower. Thus, dilatancy hardening is not likely to be very significant in geologic processes. In certain engineering applications, however, breakdown of the law of effective stress and strengthening due to dilatancy must be considered. A good example is the situation in water-saturated rock which surrounds buried nuclear explosions. There, a strengthening will probably accompany the high rates of strain imposed on the rock.

Another situation of interest might be the rock stressed as a result of earthquake motion. The events preceding an earthquake probably occur slowly enough so that critical strain rates would not be exceeded. Once rocks are set in motion, however, redistribution of stress could take place rather rapidly. Stress in rocks just ahead of the point of farthest advance of a fault could well be raised at rates which exceed the critical rates, with dilatancy hardening as a consequence. With time, pore fluids would move into such a region and re-establish the normal pore pressure. Then, strength would fall back to the normal level. Perhaps some aftershock activity would result from this lowering of strength. The time between main shock and aftershock would presumably depend on the same factors as the critical strain rate does, namely on permeability of the rock, viscosity of the pore fluid, and dimensions of the mass of stressed rock in question.

## CONCLUSIONS

We conclude that the law of effective stress is of even greater generality than had been previously realized in that it holds for crystalline rocks of low porosity as long as loading rates are kept below certain critical values. The critical rate depends not only on the particular rock but also on the fluid in the pores and geometrical factors such as distance from the center of the rock mass in question to a source of pore fluid. An estimate of the critical rate for geologic situations suggests that this rate will seldom be exceeded in the earth. One exception might be rock stressed as a result of earthquake motion. The initial dilatancy hardening with a later fall in strength as pore pressure returns to normal could produce aftershock activity. In engineering applications, particularly where high rates of loading prevail, the critical strain rate might well be exceeded; under these circumstances important departures from the law of effective stress must also be expected.

*Acknowledgements*—This work was supported by the National Science Foundation as Grant GA-613 and by Advanced Research Projects Agency under Contract DADA01-67-C-0090. J. B. Walsh and J. D. Byerlee made several helpful suggestions in the course of the experimental work and reviewed the manuscript.

## REFERENCES

1. Jaeger J. C. Brittle Fracture of Rocks, in *Failure and Breakage of Rocks* (C. Fairhurst, Ed.) AIMME, New York, pp. 3–57 (1967).
2. Robinson L. H., Jr. The effect of pore and confining pressure on the failure process in sedimentary rock. *Colo. Sch. Mines Q.* **54**, (3) 177–199 (1959).
3. Handin J., Hager R. V., Jr., Friedman M. and Feather J. N. Experimental deformation of sedimentary rocks under confining pressure: Pore pressure tests. *Bull. Am. Ass. Petrol. Geol.* **47**, 717–755 (1963).
4. Serdengecti S. and Boozer G. D. The Effects of Strain Rate and Temperature on the Behavior of Rocks Subjected to Triaxial Compression, *Proceedings of the Fourth Symposium on Rock Mechanics*, Pennsylvania State University, pp. 83–97 (1961).
5. Brace W. F., Orange A. S. and Madden T. M. The effect of pressure on the electrical resistivity of water-saturated crystalline rocks. *J. geophys. Res.* **70**, (22) 5669–5678 (1965).
6. Walsh J. B. and Brace W. F. Cracks and Pores in Rocks, *Transactions of the First International Congress on Rock Mechanics*, Lisbon, pp. 643–646 (1966).
7. Brace W. F., Walsh J. B. and Frangos W. T. Permeability of granite under high pressure. *J. geophys. Res.* **73**, (1968).
8. Heard H. C. Transition from brittle fracture to ductile flow in Solenhofen limestone as a function of temperature, confining pressure, and interstitial fluid pressure, in rock deformation. *Mem. geol. Soc. Am.* **79**, 193–226 (1960).
9. Bridgman P. W. Further rough compressions to 40,000 kg/cm² especially certain liquids. *Proc. Am. Acad. Arts Sci.* **77**, 129–146 (1949).
10. Bridgman P. W. Viscosities to 30,000 kg/cmi. *Proc. Am. Acad. Arts Sci.* **77**, 117–128 (1949).
11. Heard H. C. Effect of large changes in strain rate in the experimental deformation of Yule marble. *J. Geol.* **71**, 162–195 (1963).
12. Brace W. F., Paulding B. W., Jr. and Scholz C. H. Dilatancy in the fracture of crystalline rocks. *J. geophys. Res.* **71**, (16) 3939–3954 (1966).
13. Newman K. Properties of Concrete, in *Structural Concrete*, Vol. 2, pp. 2–34 (1956).
14. Frank F. C. On dilatancy in relation to seismic sources. *Rev. Geophys.* **3**, 484–503 (1965).
15. Martin R. J. *The Effect of Pore Pressure on the Strength of Low Porosity Crystalline Rocks*, M. S. thesis, Massachusetts Institute of Technology, September (1967).
16. Brace W. F. and Orange A. S. Electrical resistivity changes in saturated rocks during fracture and frictional sliding. *J. geophys. Res.* **73**, 1433 (1968).

17. SCHOLZ C. H. *Microfracturing of Rocks in Compression*, Ph.D. thesis, Massachusetts Institute of Technology, September (1967).
18. CARSLAW H. S. and JAEGER J. C. *Conduction of Heat in Solids*, 2nd edn., Oxford University Press (1959).

## APPENDIX

We wish to calculate the change in pore pressure within the sample just before fracture, as a function of strain rate and, from this, to estimate the amount of dilatancy hardening. Changes in pore pressure within the sample result from competing effects: pore volume increase due to stress causes a *drop* in pressure whereas flow of water to the sample from a reservoir at one end tends to *restore* the pressure to the value it had before stress was applied. The more rapidly the rock is deformed, the farther the second effect lags behind the first and the greater the resulting change in pore pressure. Calculation of the first effect, the pressure drop due to dilatant volume change, is simple. Calculation of the second is more involved and requires several approximations.

A curve of volumetric strain vs. time (Fig. 8) served as a basis of our calculation. The strains, which represent changes in porosity, were measured with strain gages [12]. The rock was stressed at a constant rate, so that the time axis is equivalent to a stress axis.

The calculation was done step by step, so the curve in Fig. 8 was first divided into increments of equal volumetric strain. At each increment two operations were performed: first the pressure drop due to dilatant

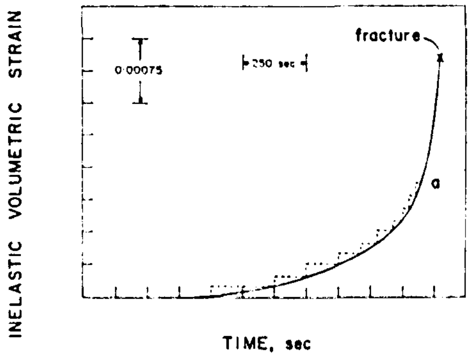


FIG. 8. Volume changes in Westerly granite as stress was applied at a constant rate. The elastic part of the volume change has been subtracted, leaving inelastic volume changes. Fracture occurred at $x$, and $a$ is the strain at 95 per cent of the fracture stress. The steps are discussed in the text.

volume change is taken from the pressure at the beginning of that increment; second, the recovery in pressure due to inflow from the reservoir at the end of the time represented by that increment was calculated. A new pressure drop was then applied to the final pressure and the recovery again calculated. This went on until the point $a$ is reached. At point $a$, stress reached about 95 per cent of the fracture stress, and several lines of evidence suggest that a well-defined fault was present [17]; permeability probably increased very markedly and further dilatancy was very likely restricted to the vicinity of the fault. The pore pressure at $a$ was assumed to be the pore pressure at faulting and it is this pressure which is given in Fig. 6.

The pressure drop due to dilatant volume change was obtained directly from $\Delta P = -\Delta V/\beta\eta$ where $\beta$ is compressibility of the pore fluid, $\eta$ is initial porosity of the sample and $\Delta V$ is an increment of volumetric strain (Fig. 8).

The degree to which pore pressure, $P$, is restored can be calculated from the following equation of flow, valid when the compressibility of the fluid is much larger than that of the rock [15]:

$$\nabla^2 P = (1/a)\, \delta P/\delta t \qquad (1)$$

where

$$a = k/\mu\beta\eta.$$

Here $k$, is the permeability of the rock and $\mu$ is fluid viscosity. Boundary conditions for our sample were assumed to be as follows. Flow of fluid was taken to be one dimensional, parallel with the axis of the sample. An infinite reservoir at constant initial pressure, $P_0$, was assumed at one end of the sample. To simplify the problem we looked at the pressure at midlength of the sample; most of the faults in our samples extended at least this far. Further, we assumed that at the end of each increment of volume change we could, as a first approximation, replace the actual pressure distribution with a constant pressure having the value of the pressure at mid-length. On this basis, a solution to (1), given by [18], is

$$P_t = P_0 + \frac{2}{L}\sum_{n=0}^{\infty} \exp\left[-\alpha (2n+1)^2 \pi^2 t/4L^2\right] \cos (2n+1)\, \pi x/2L$$
$$\{2L/(2n+1)\, \pi[(-1)^{n+1} P_0 + (-1)^n (P_{t-1} - \Delta P_t)]\} \tag{2}$$

where $P_t$ is the pressure as a function of length, at the end of each time increment, $\Delta P_t$ is the pressure increment calculated above from dilatant volume change and $P_{t-1}$ is the pressure at midlength of the preceding increment. For tests at strain rates of $10^{-4}$ sec$^{-1}$ and faster, fractures did not extend beyond the lower half of the sample. For these cases, we looked at the pressure one third of the length from the reservoir, instead of midlength.

Repeated application of (2) yielded, for a given strain rate, a value of pore pressure, $P$. The entire operation was repeated at several strain rates. Fluid permeability, $k$, was assumed to have the value found by applying the relation between $k$ and resistivity $\rho$ found by BRACE *et al.* [7],

$$k = \text{const. } \rho^{-1.5}$$

to resistivities measured as granite was stressed to fracture [16].